LAWRENCE
LIVERMORE
NATIONAL
LABORATORY

LLNL-TR-526952

Two-Stage, Integrated, Geothermal-CO2 Storage Reservoirs: An Approach for Sustainable Energy Production, CO2-Sequestration Security, and Reduced Environmental Risk

T. A. Buscheck, M. Chen, Y. Sun, Y. Hao, T. R. Elliot

February 3, 2012

Disclaimer

This work performed under the auspices of the U.S. Department of Energy by Lawrence Livermore National Laboratory under Contract DE-AC52-07NA27344.

Two-Stage, Integrated, Geothermal-CO2 Storage Reservoirs: An Approach for Sustainable Energy Production, CO_2-Sequestration Security, and Reduced Environmental Risk

Thomas A. Buscheck[a], Mingjie Chen[a], Yunwei Sun[a], Yue Hao[a], and Thomas R. Elliot[b]

[a]Lawrence Livermore National Laboratory, Livermore CA USA

[b]Department of Civil and Environmental Engineering, Princeton University, Princeton, NJ USA

Abstract

We introduce a hybrid two-stage energy-recovery approach to sequester CO_2 and produce geothermal energy at low environmental risk and low cost by integrating geothermal production with CO_2 capture and sequestration (CCS) in saline, sedimentary formations. Our approach combines the benefits of the approach proposed by Buscheck et al. (2011b), which uses brine as the working fluid, with those of the approach first suggested by Brown (2000) and analyzed by Pruess (2006), using CO_2 as the working fluid, and then extended to saline-formation CCS by Randolph and Saar (2011a). During stage one of our hybrid approach, formation brine, which is extracted to provide pressure relief for CO_2 injection, is the working fluid for energy recovery. Produced brine is applied to a consumptive beneficial use: feedstock for fresh water production through desalination, saline cooling water, or make-up water to be injected into a neighboring reservoir operation, such as in Enhanced Geothermal Systems (EGS), where there is often a shortage of a working fluid. For stage one, it is important to find economically feasible disposition options to reduce the volume of brine requiring reinjection in the integrated geothermal-CCS reservoir (Buscheck et al. 2012a). During stage two, which begins as CO_2 reaches the production wells; co-produced brine and CO_2 are the working fluids. We present preliminary reservoir engineering analyses of this approach, using a simple conceptual model of a homogeneous, permeable CO_2 storage formation/geothermal reservoir, bounded by relatively impermeable sealing units. We assess both the CO_2 sequestration capacity and geothermal energy production potential as a function of well spacing between CO_2 injectors and brine/CO_2 producers for various well patterns and for a range of subsurface conditions.

1. Introduction

In order to stabilize atmospheric CO_2 concentrations for climate change mitigation, CCS implementation must be increased by several orders of magnitude over the next two decades (Fig. 3 of IEA, 2009). Increased reliance on geothermal energy and CO_2 capture and sequestration (CCS) in deep geological formations are both regarded as a promising means of lowering the amount of CO_2 emitted to the atmosphere and thereby mitigate climate change (Socolow and Pacala, 2006). In order for widespread deployment of industrial-scale CCS to be achievable, a number of implementation barriers must be overcome: CO_2 capture cost, sequestration safety, legal and regulatory barriers, public acceptance, water-use demands from CCS operations, and pore-space competition with emerging activities, such as shale-gas production (IPCC, 2005; Court et al., 2011a; Court, 2011).

For industrial-scale CO_2 injection in saline formations, pressure buildup can be the limiting factor in the ability to store CO_2 and is the main physical drive for potential CO_2 and brine leakage, whereas geothermal energy production is often limited by pressure depletion. Using active reservoir management, these two complementary systems can be integrated synergistically (Figure 1), with CO_2 injection providing pressure support to maintain the productivity of geothermal wells, while the net loss of brine provides pressure relief and improved injectivity for the CO_2-injection wells, thereby increasing CO_2 storage and reducing the risk of CO_2 and brine leakage (Buscheck 2010; Buscheck et al., 2011b).

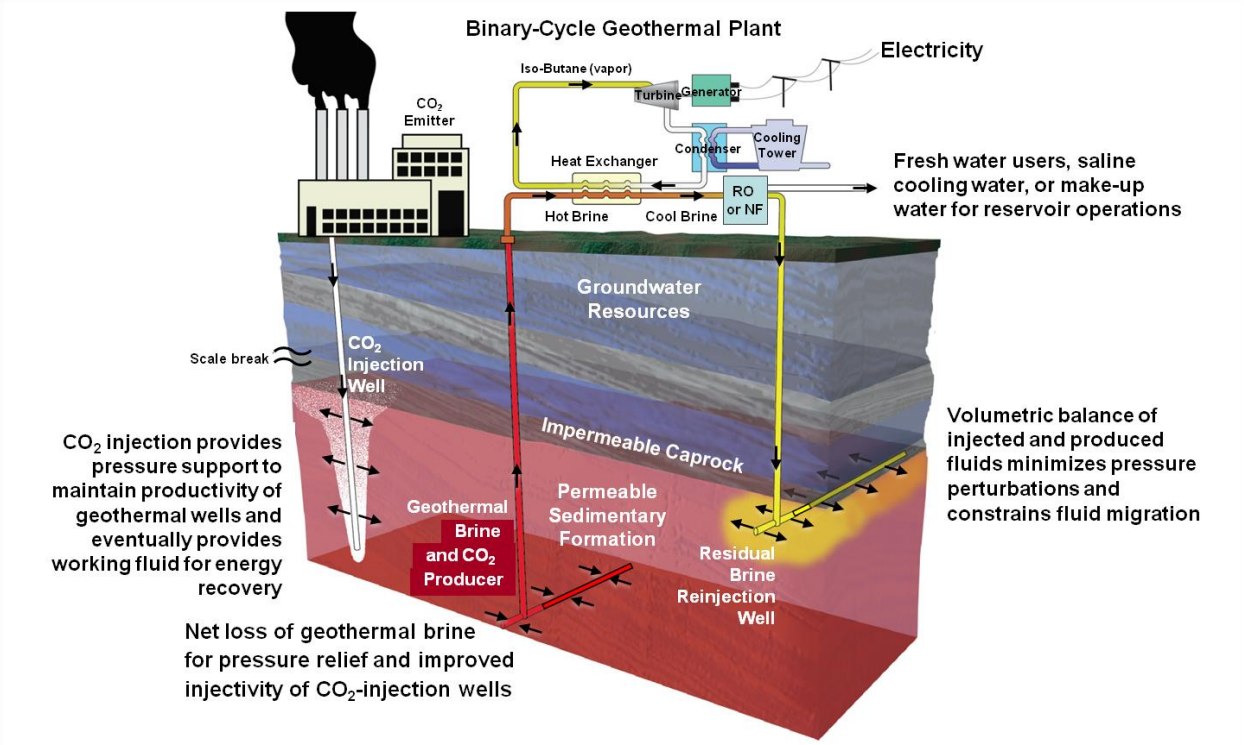

Figure 1. An actively managed, two-stage, integrated geothermal–CCS system, using binary-cycle power generation, is shown in a saline, permeable, sedimentary formation.

2. Background

Sedimentary formations are second only to crystalline basement rock in the U.S. geothermal resource base (MIT, 2006). Compared to basement rock, sedimentary formations have the advantages of higher permeability and reservoir flow capacity, without requiring hydraulic fracturing. However, sedimentary formations typically have reduced vertical permeability, caused by impermeable layers (e.g., shale) being sandwiched between permeable layers (e.g., sandstone). Sedimentary formations suitable for CCS must be overlain by an areally extensive impermeable caprock to limit the buoyancy-driven upward flow of CO_2. An impermeable caprock is also useful for geothermal reservoirs, to prevent recharge from cooler overlying formations. Reduced vertical permeability limits natural hydrothermal convection and the recharge of hot brine from below. For such systems, two approaches can allow commercially attractive flow rates: (1) vertical wells penetrating a sufficient number of permeable layers or (2) multilateral wells completed over a sufficiently long interval of permeable rock. The question of what constitutes commercially attractive flow rates depends on formation temperatures and the intended economic lifetime of heat recovery operations. A significant portion of the U.S. geothermal resource base residing in sedimentary formations is associated with relatively low geothermal heat flux (Blackwell and Richards, 2004). To attain sufficiently high temperatures in such geologic settings, it is necessary to drill to great depths. Moreover, well drilling, completion, and maintenance costs make up a substantial percentage of the capital and operating costs associated with geothermal energy production, particularly when great formations depths are involved. As discussed later, our approach may allow much greater well spacing between injectors and producers, which would provide a greater thermal footprint over which heat is harvested, compared to conventional geothermal systems (Buscheck et al., 2012c; Elliot et al., 2012). Greater well spacing would better leverage the large capital and operating costs associated with very deep wells. A large thermal footprint would result in a smaller heat extraction rate, relative to the geothermal heat flux, than in conventional geothermal systems, with the added value of reduced thermal drawdown.

More sustainable energy production increases the economic lifetime of the geothermal well field, which also would provide better leveraging of the large capital and operating costs of the well infrastructure.

As discussed later, spacing between injectors and producers is influenced by hydraulic communication, which facilitates pressure interference, between the wells. The primary reservoir factors affecting how far apart injectors and producers can be spaced from each other are (1) reservoir permeability, with larger horizontal permeability favoring increased well spacing and (2) reservoir heterogeneity and compartmentalization, arising from the presence of sedimentary baffling, sealing faults at depth, and intra-fault block heterogeneity, with greater compartmentalization generally necessitating decreased well spacing.

3. CO_2 Capture, Utilization, and Sequestration: Turning CO_2 into a Resource

The challenges of mitigating global climate change and generating sustainable energy are inseparable and require innovative, cross-cutting thinking that aggressively seeks synergistic opportunities in an open-minded manner. With the exception of CO_2-enabled Enhanced Oil Recovery (EOR), the CCS community has largely viewed CO_2 as a waste to be safely disposed of. Whereas the geothermal community, which conventionally applies brine-based heat extraction, has only recently considered CO_2 as a working fluid, with CO_2 sequestration being an ancillary benefit, rather than a strategic priority. Our goal is to develop a cross-cutting approach, which can eventually be economically deployed nationwide, that balances the priorities of (1) large-scale CO_2 sequestration, (2) sustainable geothermal energy production, and (3) minimized environmental risks. An ancillary benefit of our approach is that it also generates substantial quantities of water for beneficial use, which can be very significant in regions where water scarcity is an issue. Thus, our goal is to change the perception of CO_2 from: *waste requiring safe disposal* to: a *valuable resource* that enables economically attractive and sustainable energy production.

3.1 Active CO_2 Reservoir Management

For industrial-scale CO_2 injection in saline formations, pressure buildup is a limiting factor in CO_2 sequestration capacity and risk mitigation because it drives CO_2 and brine migration (Birkholzer and Zhou, 2009). As a means to mange pressure buildup and to control CO_2 and brine migration, Lawrence Livermore National Laboratory (LLNL) and Princeton University have been collaborating on the development of Active CO_2 Reservoir Management (ACRM), which combines brine extraction and treatment and residual-brine reinjection with CO_2 injection (Buscheck et al., 2011a, 2012a, 2012b; Court et al., 2011b, 2012; Court, 2011). This concept is being considered for specific CCS sites in the state of Wyoming (Surdam et al., 2009) and off the coast of Norway (Bergmo et al., 2011). Combining brine extraction/treatment and residual-brine reinjection with CO_2 injection causes "push-pull" manipulation of the CO_2 plume, which exposes *less* of the caprock seal to CO_2 and *more* of the storage formation to CO_2, with a greater fraction of the formation utilized for trapping. Because ACRM increases CO_2 sequestration capacity and reduces brine migration, the area required for securing property rights is reduced. If the net extracted volume of brine is equal to the injected CO_2 volume, pressure buildup is minimized in magnitude, temporal, and spatial extent, reducing the Area of Review (AOR) by as much as two orders of magnitude, reducing the duration of post-injection monitoring, as well as reducing the risks of induced seismicity, fault activation, and leakage up abandoned wells (Buscheck et al., 2011b, 2012a, 2012b). Moreover, a reduction in pressure perturbation magnitude and extent will lower the volume of brine migration. Minimized pressure perturbations also reduce pore-space competition with other subsurface activities, such as shale gas (Elliot and Celia, 2012; Buscheck et al., 2012b).

Extracted brine is available as a feedstock for desalination, such as Reverse Osmosis (RO). Depending on formation temperature, geothermal heat recovered from the produced brine and CO_2 can generate enough electricity to defray the costs of CCS. Geothermal heat recovery is also beneficial for RO treatment, because

the operating lifetime of RO membranes is greater when temperature is less than 40-50^{o}C (Aines et al., 2010). It has been suggested (Surdam et al., 2009) that the proposed CO_2 sequestration site at the Rock Springs Uplift in Wyoming, with formation temperatures ranging from 100 to 130^{o}C, may be suitable for geothermal energy production. ACRM is being considered by the State of Wyoming for this site, where it is estimated that injecting 15 million tons of CO_2 annually into the Weber Sandstone could yield 10,000 acre-feet of potable water per year, based on the assumption that the ratio of produced fresh water to RO-treated brine is 0.9 and the residual brine would be reinjected into a separate formation (Surdam et al., 2009).

The feasibility of brine extraction is constrained by brine composition and treatability (Aines et al. 2010; Bourcier et al., 2011). Treatment becomes more difficult (and expensive) with increasing total dissolved solids (TDS), which ranges from a lower (regulatory) limit of 10,000 mg/L up to about 400,000 mg/L. Brines with TDS in the range 10,000-40,000 mg/L are prime candidates for RO treatment, using a process much like that for seawater for which a large industry currently exits. Brines with TDS in the range 40,000-85,000 mg/L may be treatable by RO alone, but with lower recovery. Above 85,000 mg/L, less conventional methods are necessary, such as nanofiltration (NF) and subsequently RO or multi-stage RO. Above 300,000 mg/L, brines are considered economically untreatable. Data for various western states (e.g., Colorado, Wyoming, and California) show substantial areas where brine is in the 10,000-85,000 mg/L range, indicating that ACRM is feasible, with respect to brine TDS and composition.

The feasibility of using brine as saline cooling water is also constrained by brine composition and treatability. There is an expanding industrial experience base in the use of saline cooling water. One sector (Maulbetsch and DiFilippo, 2010) consists of otherwise conventional power plants that use estuarine water or seawater in slightly oversized cooling towers. The second sector (Duke, 2007) consists of power plants that utilize the "zero liquid discharge" (ZLD) concept, in which no residual liquid is returned to the original source. ZLD attempts to vaporize a large fraction of the water in the cooling process by making a large number of cycles so as to minimize the amount of blowdown for final disposal.

3.2 CO_2 EGS and CO_2-Plume Geothermal (CPG) Systems

A Hot Dry Rock geothermal energy (EGS) concept utilizing CO_2 instead of water as the working fluid was first suggested by Brown (2000) and would achieve geologic sequestration of CO_2 as an ancillary benefit. Pruess (2006) followed up on his suggestion by evaluating thermophysical properties and performing reservoir simulations. Pruess (2006) analyzed a five-spot pattern with four CO_2 injectors and a producer in the center, with 707-m spacing between the producer and injectors and found CO_2 to be superior to water in mining heat from hot fractured rock, including a reduced parasitic power consumption to drive the fluid circulation system. This concept has been extended to CCS in saline, sedimentary formations (Randolph and Saar, 2011a). They observed that EGS typically requires hydraulic fracturing Hot Dry Rock, which runs the risk of induced seismicity and undesirable hydraulic communication. Hence, EGS has met social-political resistance, including termination of EGS projects, such as in Basel, Switzerland (Glanz, 2009). Randolph and Saar (2011a, 2011b) have analyzed this approach applied to sedimentary formations, which they call a CO_2-Plume Geothermal (CPG) system, to distinguish their approach from CO_2-enabled EGS. For their reservoir analyses, they use the same five-spot well configuration as analyzed by Pruess (2006). With respect to parasitic energy costs for driving the fluid circulation system, Randolph and Saar (2011b) found CO_2 to be more efficient than water and brine for low-to-moderate permeability ($k < 2\times10^{-14}$ to 2×10^{-13} m^2).

4. Two-Stage, Integrated Geothermal-CCS Approach

The determination of the feasibility of deploying actively managed integrated, two-stage, geothermal-CCS at a given site depends on several primary factors (Figure 2a), including:

- **Formation with sufficient CO_2 storage/trapping characteristics**: (1) storage-formation volume, permeability, porosity, and depth, (2) caprock "seal" thickness, areal extent, and sufficiently low permeability, and (3) remoteness from potable-water aquifers and the atmosphere
- **Brine disposition options:** brine salinity and composition influence the feasibility of various brine treatment options, as does proximity to water consumers, such as other reservoir operations
- **Formation temperature**: affecting energy production rate per unit mass of extracted brine
- **Proximity to CO_2 emitters:** affecting CO_2 conveyance costs via pipelines (Note that conveyance cost and feasibility is influenced by current and planned infrastructure and demographics.)
- **Competition for pore space:** which includes natural gas storage, liquid waste disposal, shale gas, and other uses (Elliot and Celia, 2012; Court et al., 2012; Court, 2011)
- **Regulatory and demographic constraints:** which can vary from state to state

If all of these attributes pertain to a single CO_2 reservoir, Buscheck et al. (2011b) has named this *single-formation* ACRM (Figure 2). ACRM may also be deployed using separate formations in "tandem", with one formation being utilized for CO_2 storage and a separate formation being utilized for the purpose of brine reinjection (Figure 3). *Tandem-formation* ACRM involves two or more formations that may possess less than all of the attributes listed above (Buscheck et al., 2011b). For example, a formation with excellent CO_2 storage/trapping characteristics and good proximity to CO_2 emitters could be used in tandem with a formation with marginal CO_2 storage/trapping characteristics, low-salinity brine that could be treated at low cost, and possibly high formation temperature. Brine extracted from the first (CO_2-storage) formation would be conveyed (via pipeline) and injected into the second (brine-storage) formation. Extraction of native brine from the second formation would be put through a binary-cycle geothermal plant and treated, using RO, which would produce fresh water and geothermal energy at relatively low cost. The residual brine would then be reinjected back into the second (brine-storage) formation. The net reduction of brine resulting from RO treatment creates pore space in the second (brine-storage) formation to allow room for brine conveyed from the first (CO_2-storage) formation to be stored there. If the temperature in the first (CO_2-storage) formation is sufficiently high, geothermal energy could also be produced from that formation (Figure 3a). Another form of tandem-formation ACRM involves conveying the produced brine to a geothermal reservoir (Figure 3b), either a conventional hydrothermal or EGS reservoir, where it would be used as make-up water, or, in the case of EGS, as the hydraulic-fracturing and working fluids as well (Harto and Veil, 2011; Bourcier et al., 2012; Buscheck et al., 2011b).

Substantial geothermal well flow rates are possible with ACRM-CCS associated with coal power plants. If the net extracted volume of brine is equal to the injected CO_2 volume, and the extracted brine is not reinjected back into the same formation, a brine production rate of ~380 kg/sec is required for the volume of CO_2 to be sequestered for a 1-GWe coal power plant. Figure 4 plots the binary-cycle geothermal power output for those conditions, when brine is used as the working fluid, as proposed by Buscheck (2010). When CO_2 is the working fluid, energy recovery will be similar to that shown in Figure 4, with the advantage of reduced parasitic power consumption to drive the fluid recirculation system (Pruess, 2006; Randolph and Saar, 2011a, 2011b).

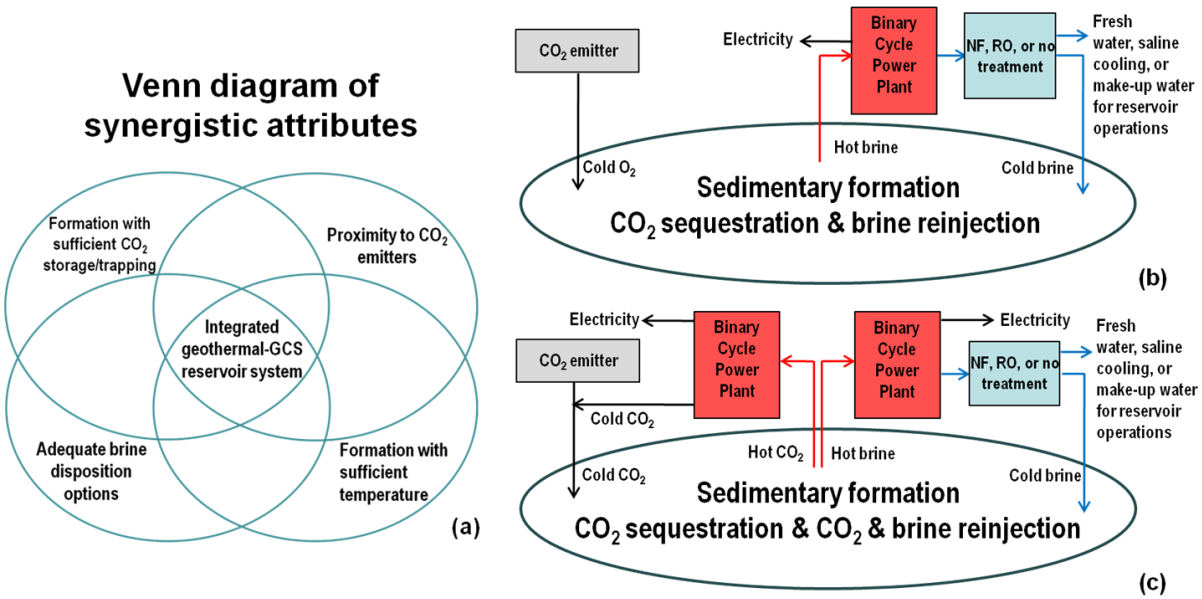

Figure 2. (a) Venn diagram showing the synergistic attributes used to determine the deployment potential of integrated geothermal-CCS systems. Schematics for *single-formation* ACRM are shown for (b) stage one and (c) stage two of a two-stage, integrated geothermal-CCS system. Note that as originally proposed by Buscheck (2010), energy harvesting did not include stage 2, which is when CO_2 becomes a co-produced working fluid, along with brine.

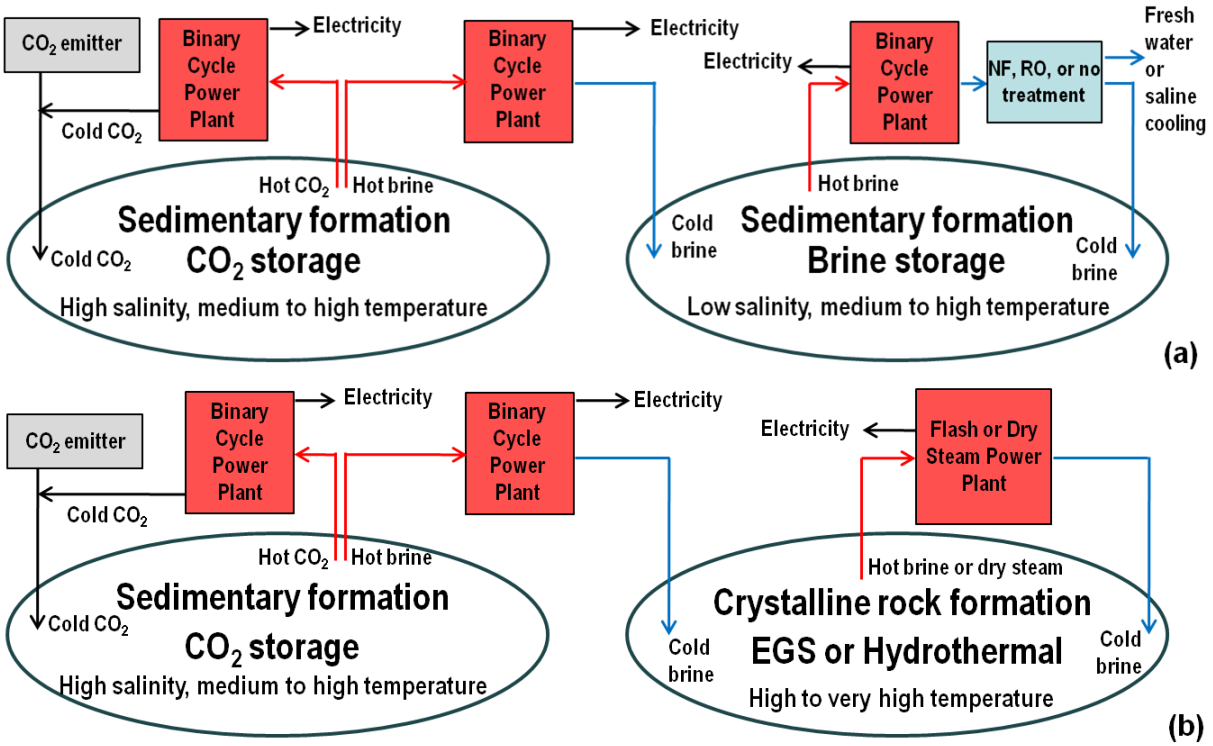

Figure 3. Schematics of *tandem-formation* ACRM with (a) binary-cycle power from stage two in the CO_2 storage reservoir and from stage one in the brine-storage reservoir and (b) *tandem-formation* ACRM with binary-cycle power from stage two of integrated geothermal-CCS in the CO_2 storage reservoir and either flash or dry steam geothermal power from the brine-storage reservoir in crystalline rock. Note that stage one heat recovery will occur prior to the CO_2 breakthrough at the production wells.

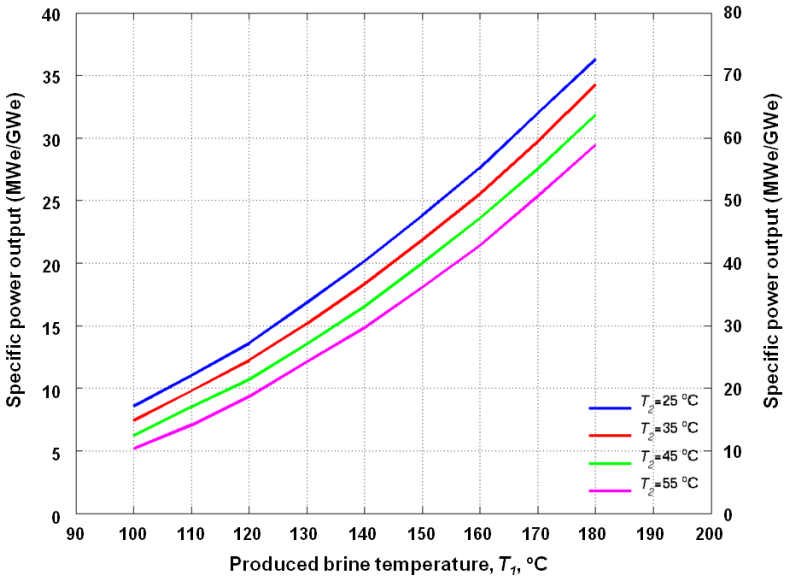

Figure 4. Specific geothermal power output per GWe of pulverized-coal-fired power generation, when the net extracted volume of brine is equal to the injected CO_2 volume and none of the produced brine is reinjected into the same formation. This plot was obtained by taking Figure 7.3 of MIT (2006), multiplying by 380 kg/s, and dividing by 1000 KWe/MWe. Note that if half of the produced brine is reinjected into the same formation, then the brine production rate would double, and the specific power output is given by the vertical axis on the right.

5. Model Methodology

In this study, we used the NUFT (Nonisothermal Unsaturated-saturated Flow and Transport) code, which was developed at Lawrence Livermore National Laboratory (LLNL) to simulate multi-phase multi-component heat and mass flow and reactive transport in unsaturated and saturated porous media (Nitao, 1998; Buscheck et al., 2003; Johnson et al., 2004a, 2004b; Carroll et al., 2009; Morris et al., 2011). The pore and fluid compressibility are 4.5×10^{-10} and 3.5×10^{-10} Pa^{-1}, respectively. Water density is determined by the ASME steam tables (ASME, 2006). The two-phase flow of CO_2 and water was simulated with the density of supercritical-CO_2 determined by the correlation of Span and Wagner (1996) and viscosity determined by the correlation of Fenghour et al. (1997).

We used a 3-D model with quarter symmetry to represent a 250-m-thick storage formation (reservoir), similar to that modeled by Zhou et al. (2008) and Buscheck et al. (2011a), with the top of the reservoir located either 2250 or 4750 m below the ground surface, bounded by relatively impermeable 100-m-thick seal units. Thus, the bottom of the reservoir is at 2500 and 5000 m depths. Note that the model used in Section 6.1 required 79,524 grid blocks (Figure 5). The outer boundaries have a no-flow condition to represent a semi-closed system for reservoir area of 1257 km^2 for the 12 and 16 well configurations analyzed in Section 6.1. The lower boundary, located 1000 m below the bottom of the reservoir, has a no-flow condition and a specific geothermal heat flux of either 50, 75, or 100 mW/m^2 in Section 6.1. Because we used an average thermal conductivity of 2.0 W/m^oC, this results in thermal gradients of 25, 37.5 and $50^oC/km$. For the 5-spot well patterns (Section 6.2), the bottom of the reservoir is at 2500 m depth and the geothermal heat flux is 75 mW/m^2. Hydrologic properties (Table 1) are similar to previous studies (Zhou et al., 2008; Buscheck et al., 2011a, 2011b, and 2011c). CO_2 injection and fluid (brine plus CO_2) production occur in the lower half of the reservoir. For all cases we maintained a fluid mass balance between injected CO_2 and produced fluids. Because supercritical CO_2 is approximately 30 percent less dense than water, this results in a small overpressure in the reservoir during the time when brine production predominates. CO_2 is injected at a fluid enthalpy corresponding to 16.0^oC at injection conditions, which approximates average annual surface temperatures.

Table 1. Hydrologic property values used in the study are listed.

Property	Storage formation	Caprock seal
Horizontal and vertical permeability (m^2)	1.0×10^{-13}	1.0×10^{-18}
Pore compressibility (Pa^{-1})	4.5×10^{-10}	4.5×10^{-10}
Porosity	0.12	0.12
van Genuchten (1980) *m*	0.46	0.46
van Genuchten α (Pa^{-1})	5.1×10^{-5}	5.1×10^{-5}
Residual supercritical CO_2 saturation	0.05	0.05
Residual water saturation	0.30	0.30

6. Results

6.1 Analyses of 12 and 16 Well Patterns

As originally proposed by Buscheck (2010), the focus of integrated geothermal-ACRM-CCS was to optimize the storage of CO_2. Therefore, it was thought to be necessary to avoid, or at least delay, the breakthrough of CO_2 at the producers to maximize the useful lifetime of the brine producers (Buscheck et al., 2011b, 2012a). Pressure relief from brine production increases with decreasing spacing between the CO_2 injectors and brine producers, while CO_2 breakthrough time increases with well spacing. Therefore, reservoir analyses focused on the tradeoff between achieving pressure relief, while delaying CO_2 breakthrough. Various approaches were investigated, such as the use of horizontal wells and successively producing brine from a series of producers incrementally spaced farther from the injector. The use of "smart-wells" was suggested, but not analyzed, with down-hole sensors and multiple independently-controlled production and injection zones to extend the useful lifetime of brine producers. For vertical wells, this involved concentric rings of brine producers. Because of the large areal scales involved, it appeared that it could be difficult to build a pipeline network to bring the hot brine to a central geothermal plant. Thus, we decided to turn our original concept "inside-out", with CO_2 injectors on the outer perimeter and producers clustered in the center. Figure 5 shows the growth of the CO_2 plume for a ring of 8 CO_2 injectors, 10 km from the center and an inner ring of producers, 2 km from the center. It was found that producing from the center is an effective means of controlling the influence of buoyancy on CO_2 plume migration, substantially increasing the utilization of the CO_2 storage formation (Buscheck et al., 2012c; Elliot et al., 2012). These reservoir performance benefits reduce pore-space competition and pressure interference with neighboring subsurface activities, such as shale gas, and can help streamline the permitting process.

Because 190 kg/sec is higher flow rate than typically found in geothermal production wells, we modified the case shown in Figure 5, by increasing the number of producers to 8, with each located 3 km from the center of the injection zone. We moved the producers farther from the center to reduce the pressure drawdown. Note that the injectors and producers are completed in the lower half of the 250-m-thick storage formation. The geothermal and CO_2-sequestration performance of this 16-well configuration is shown in Figure 6. Production well temperature histories show a very small decrease during early time, which corresponds to cooler water from the upper half of the storage formation being drawn into the producers. Thus, the temperature decline during the first 30 yr is the result of thermal mixing. For these cases, the CO_2 front reaches the production wells sometime between 30 and 100 yr (Figure 6b, Table 2); hence, the small temperature decline during that timeframe corresponds to the arrival of the slightly cooler CO_2 plume. After CO_2 breakthrough, thermal conduction from the large thermal footprint, compared to typical geothermal reservoir systems, prevents further decline of temperatures in the CO_2 plume. Hence, the natural geothermal gradient is able to replenish the heat removed from the convection zone between the injectors and producers.

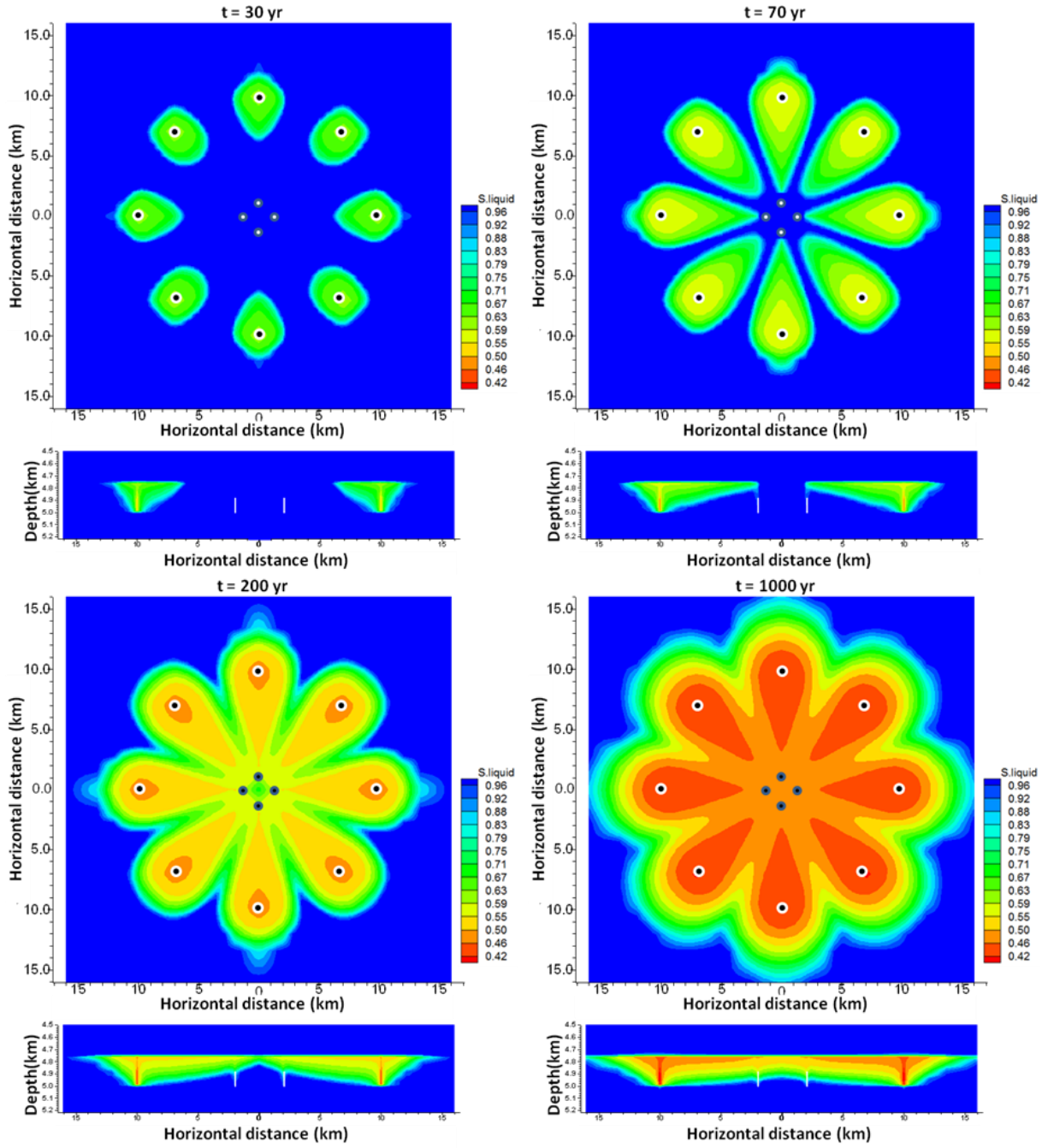

Figure 5. Liquid saturation is plotted for a 8 CO_2 injectors, 10 km from the center and 4 producers, 2 km from the center at (a) 70 yr, shortly after CO_2 breakthrough occurs, and (b) 1000 yr for a total CO_2 injection rate of 760 kg/sec and total fluid (brine plus CO_2) production rate of 760 kg/sec. The reservoir is 4750 to 5000 m deep, with a permeability of 1 x 10^{-13} m^2, bounded by 100-m-thick seal units with permeability of 1 x 10^{-18} m^2; all with 12 percent porosity and a thermal conductivity of 2.0 W/m^{o}C. The wells are completed in the lower half of the reservoir.

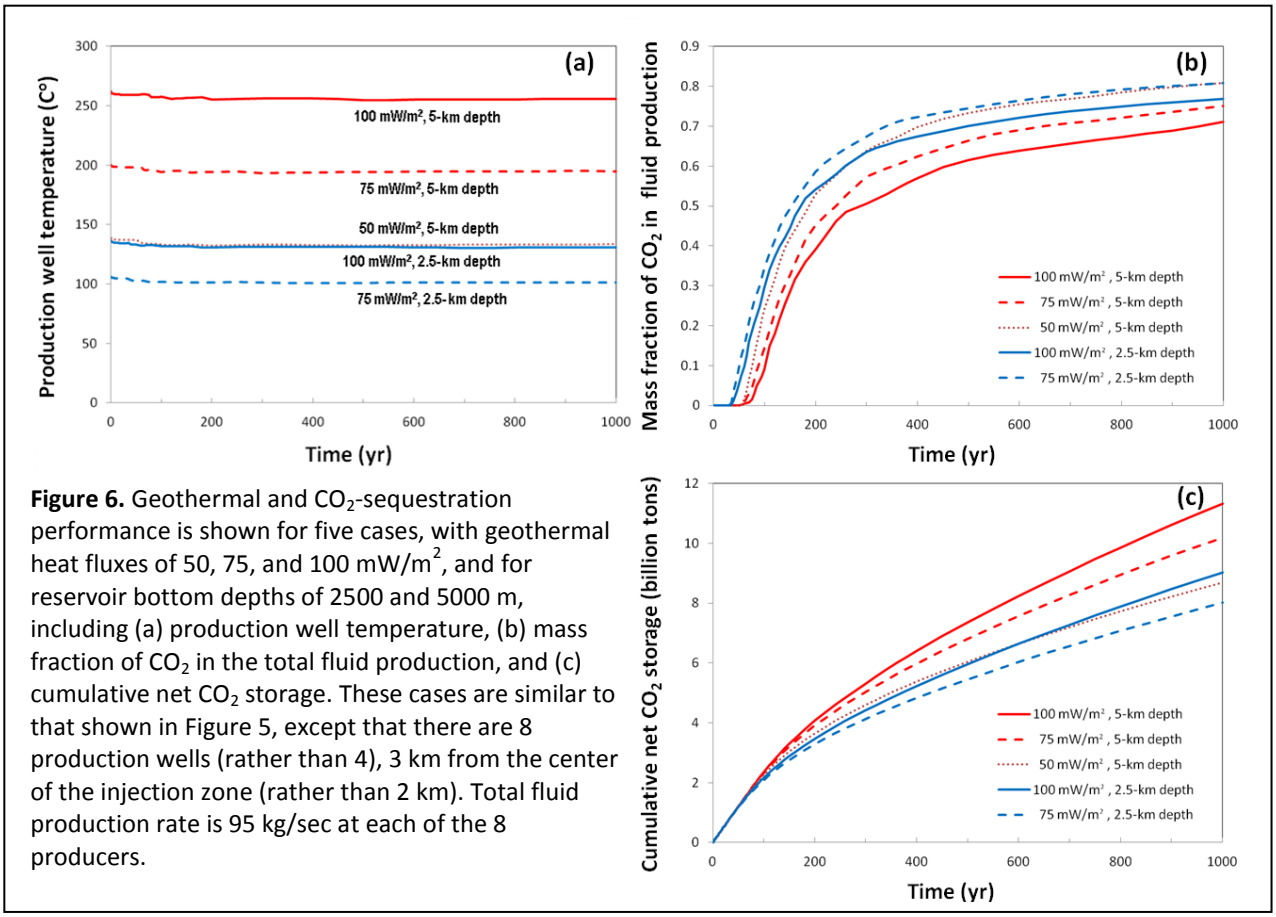

Figure 6. Geothermal and CO_2-sequestration performance is shown for five cases, with geothermal heat fluxes of 50, 75, and 100 mW/m^2, and for reservoir bottom depths of 2500 and 5000 m, including (a) production well temperature, (b) mass fraction of CO_2 in the total fluid production, and (c) cumulative net CO_2 storage. These cases are similar to that shown in Figure 5, except that there are 8 production wells (rather than 4), 3 km from the center of the injection zone (rather than 2 km). Total fluid production rate is 95 kg/sec at each of the 8 producers.

Table 2. Production well temperature histories are summarized for the 16-well pattern cases (Figure 6).

Geothermal heat flux (mW/m^2)	Reservoir bottom depth (m)	Production temperature (°C)				Thermal drawdown (°C)[a]	
		0 yr	30 yr	100 yr	1000 yr	100 yr	1000 yr
50	5000	138	137	133	133	4	4
75	5000	200	198	194	195	4	3
100	5000	262	259	257	256	2	3
75	2500	137	134	132	131	2	3
100	2500	106	104	102	101	2	3

[a]Thermal drawdown is determined relative to the temperature at 30 years, because the initial temperature decline is caused by drawing cooler brine from the upper half of the reservoir.

CO_2-sequestration performance of this 16-well configuration is summarized in Table 3. The annual CO_2 injection rate is nearly 24 million tons per year for the 8 CO_2 injectors, which is the CO_2 generated by 3 GWe of coal-fired electrical power. Prior to CO_2 breakthrough at the producers, the cumulative net CO_2 storage increases linearly (Figure 6c). At 30 years, the net cumulative CO_2 storage is 720 million tons. In contrast, the CPG concept, which emphasizes the recirculation of CO_2, does not result in large net storage of CO_2. The five-spot well configuration, analyzed to demonstrate CPG, only resulted in 20 million tons of cumulative net storage after 25 years of injection at 280 kg/sec (Randolph and Saar, 2011a). When achieving early recirculation of CO_2 as a working fluid is the focus of CO_2 injection, this will not result in significant CO_2 sequestration, relative to the global need for climate change mitigation. At 100 yr, our 16-well configuration has sequestered greater than 2 billion tons of CO_2, two orders of magnitude greater than in the CPG example analyzed by Randolph and Saar (2011a). Our approach intentionally balances the need for permanent CO_2 sequestration with the use of CO_2 as an efficient working fluid for geothermal heat recovery. The ancillary benefit of sequestering huge volumes of CO_2 is that it creates an enormous thermal footprint wherein geothermal heat can be efficiently and more sustainably harvested.

Table 3. CO_2-sequestration performance for the 16-well pattern is summarized.

Geothermal heat flux (mW/m^2)	Reservoir bottom depth (m)	Cumulative net CO_2 storage (billion tons)					
		0 yr	30 yr	100 yr	200 yr	500 yr	1000 yr
50	5000	0.0	0.72	2.26	3.64	6.04	8.68
75	5000	0.0	0.72	2.32	3.90	6.81	10.2
100	5000	0.0	0.72	2.36	4.06	7.35	11.3
75	2500	0.0	0.72	2.09	3.28	5.96	8.02
100	2500	0.0	0.72	2.16	3.46	5.46	9.03

6.2 Analyses of 5-Spot Well Patterns

The 12 and 16 well patterns analyzed in Section 6.1 are not typical of those used in petroleum fields. We decided to analyze 5-spot well patterns, which are typically used in petroleum field operations for injecting water and CO_2 during secondary and tertiary (EOR) recovery operations. A production well is surrounded by four "corner" CO_2 injectors. Because this pattern is repeated over a large well field, each production well receives the fluid injection from one-fourth of the injection rate of each of the corner wells. This allows the quarter symmetry model to end at the no-flow boundaries between each of the repeated 5-spot well patterns. Thus, the thermal footprint for each production well is equal to the area circumscribed by the four "quarter" injectors. We analyzed well configuration areas of 1, 2, 4, 8, and 16 km^2, with well spacings of 0.7071, 1.0, 1.4142, 2.0, and 2.8284 km, respectively, between the producer and 4 corner CO_2 injectors. Fluid production rate is 120 kg/sec, which is achievable using conventional down-hole pumps. The CO_2 injection rate is 30 kg/sec for each of the corner injectors, with the remaining 90 kg/sec going to the adjoining 5-spot patterns.

Before we consider the suite of 5-spot cases, we first consider a case analyzed by Randolph and Saar (2011a) who considered a 5-spot pattern with 0.7071-km well spacing, a reservoir thickness of 305 m, and 280 kg/sec flow rates for the corner CO_2 injectors and the producer. The geothermal and CO_2-sequestration performance is plotted in Figure 7, and summarized in Tables 4 and 5. Saar and Randolph (2011a) determined an economic life of 25 years for this operation. In our corresponding simulation, thermal drawdown at 25 years is becoming significant, with production temperature declining to 92.5 and 85.1°C at 25 and 30 years respectively, indicative of uneconomic temperatures. When the injectors and producers are closely spaced, CO_2 quickly breaks through to the producer, resulting in little permanent CO_2 storage. Saar and Randolph (2011a) estimated that only 7 percent of the injected CO_2 is not recovered (i.e., permanent storage) during the lifetime (25 years) of CPG operations, while in our corresponding model, the net storage is 5.5 percent of the injected CO_2; hence, our respective simulations are in excellent agreement, both with regards to temperature history and net CO_2 storage. When the injection and production flow rates are reduced to 120 kg/sec, thermal drawdown is significantly delayed, doubling the economic lifetime of the heat recovery operations (50 versus 25 years), and doubling the net CO_2 storage to 11.1 percent of injected CO_2 at 25 years (Table 5).

Table 4. Production well temperature histories are summarized for a 5-spot well pattern with 0.7071-km well spacing (Figure 7).

Flow rate (kg/sec)	Reservoir thickness (m)	Production temperature (°C)							Thermal drawdown (°C)[a]				
		0 yr	5 yr	10 yr	25 yr	30 yr	50 yr	100 yr	20 yr	25 yr	30 yr	50 yr	100 yr
280.0	305.0	106.0	103.0	102.0	92.5	85.1	55.3	28.5	4.3	10.5	17.9	47.7	74.5
120.0	250.0	106.0	103.0	103.0	102.0	102.0	91.4	54.8	1.0	1.0	1.0	11.6	48.2

[a]Thermal drawdown is determined relative to the temperature at 5 and 10 years, because the initial temperature decline is caused by drawing cooler brine from the upper half of the reservoir. For the 280.0 kg/sec case, CO_2 breakthrough occurs before thermal mixing is complete.

Table 5. CO_2-sequestration performance is summarized for a 5-spot well pattern with 0.7071-km well spacing (Figure 7).

Flow rate (kg/sec)	Reservoir thickness (m)	Cumulative net CO_2 storage (million tons)						
		0 yr	25 yr	30 yr	100 yr	200 yr	500 yr	1000 yr
280.0	305.0	0.0	12.1	12.4	13.5	14.2	15.5	16.5
120.0	250.0	0.0	11.2	11.5	12.6	13.2	14.1	14.8

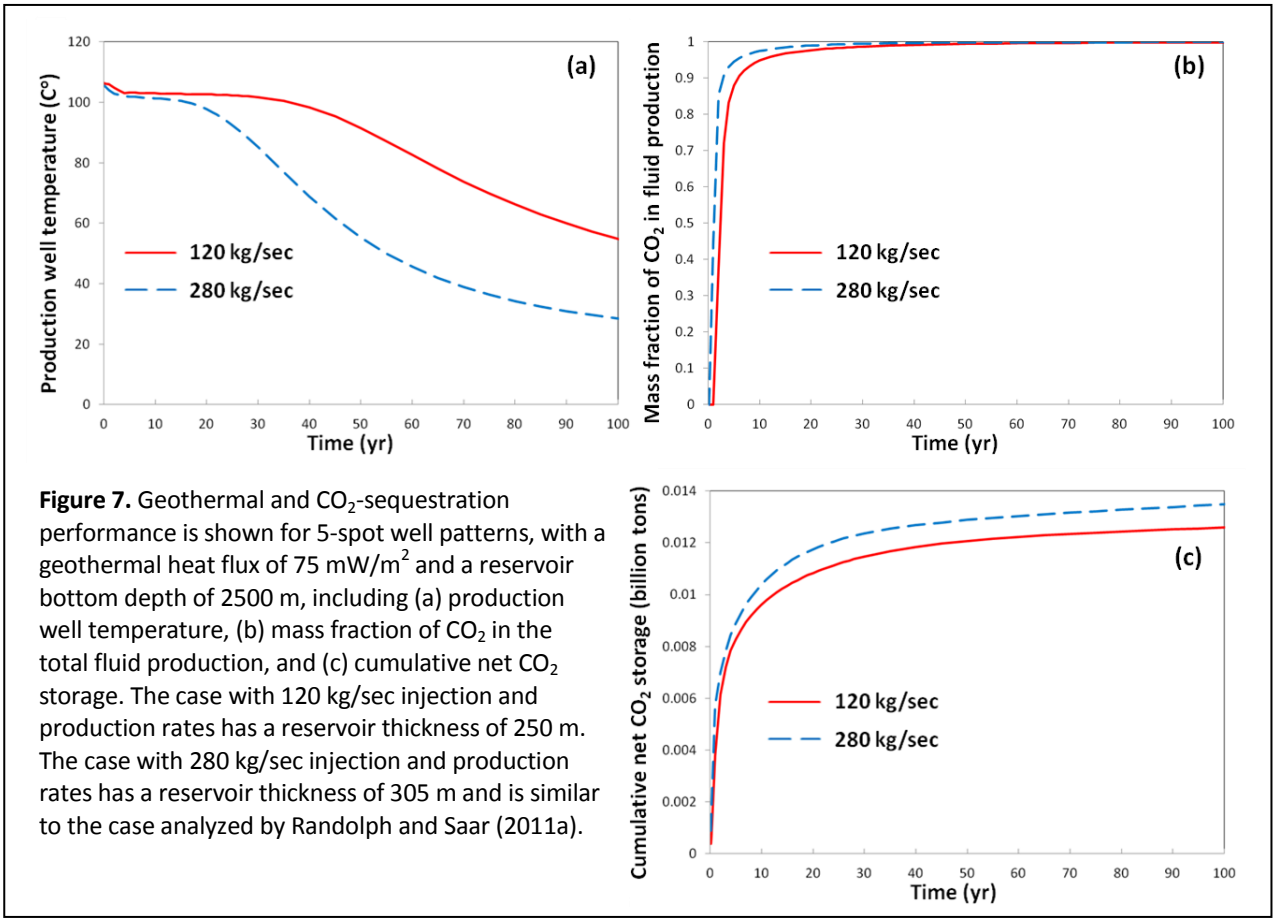

Figure 7. Geothermal and CO_2-sequestration performance is shown for 5-spot well patterns, with a geothermal heat flux of 75 mW/m^2 and a reservoir bottom depth of 2500 m, including (a) production well temperature, (b) mass fraction of CO_2 in the total fluid production, and (c) cumulative net CO_2 storage. The case with 120 kg/sec injection and production rates has a reservoir thickness of 250 m. The case with 280 kg/sec injection and production rates has a reservoir thickness of 305 m and is similar to the case analyzed by Randolph and Saar (2011a).

Geothermal and CO_2-sequestration performance of the 5-spot well pattern suite is plotted in Figures 9 and 10, and summarized in Tables 6 and 7. The economic lifetime of heat recovery operations increases with well spacing. Using the same criteria for economic lifetime used above (Table 4), with respect to thermal drawdown, the economic lifetime for these cases is 50, 100, 200, 430, and 950 years for well spacings of 0.7071, 1.0, 1.4142, 2.0, and 2.8284 km, respectively (Tables 6). Hence, economic lifetime is nearly linearly proportional to the area of the thermal footprint, indicating the influence of the geothermal heat flux.

Table 6. Production well temperature histories for are summarized for 5-spot well patterns in Figure 8.

Well spacing (km)	Area of thermal footprint (km^2)	Production temperature (°C)							Thermal drawdown (°C)[a]			
		0 yr	10 yr	30 yr	50 yr	100 yr	200 yr	1000 yr	50 yr	100 yr	200 yr	1000 yr
0.7071	1	106.0	103.0	102.0	91.4	54.8	33.6	22.2	11.6	48.2	69.4	80.8
1.0	2	106.0	103.0	102.0	102.0	92.0	57.2	28.0	1.0	11.0	45.8	75.0
1.4142	4	106.0	103.0	102.0	102.0	102.0	92.8	40.6	1.0	1.0	10.2	61.4
2.0	8	106.0	103.0	102.0	102.0	102.0	102.0	63.5	1.0	1.0	1.0	39.5
2.8284	16	106.0	103.0	102.0	102.0	102.0	102.0	90.9	1.0	1.0	1.0	12.1

[a]Thermal drawdown is determined relative to the temperature at 10 years, because the initial temperature decline is caused by drawing cooler brine from the upper half of the reservoir. The thermal drawdown is 10.2°C at 430 years for 2.0-km well spacing and 10.6°C at 950 years for 2.8284-km spacing.

Table 7. CO_2-sequestration performance is summarized for 5-spot well patterns in Figure 8.

Well spacing (km)	Area of thermal footprint (km^2)	Cumulative net CO_2 storage (million tons)					
		0 yr	30 yr	100 yr	200 yr	500 yr	1000 yr
0.7071	1	0.0	11.5	12.6	13.2	14.1	14.8
1.0	2	0.0	24.2	27.3	28.4	30.4	31.7
1.4142	4	0.0	46.4	55.1	58.2	62.6	65.8
2.0	8	0.0	73.8	105.0	115.0	125.0	133.0
2.8284	16	0.0	97.6	177.0	214.0	248.0	267.0

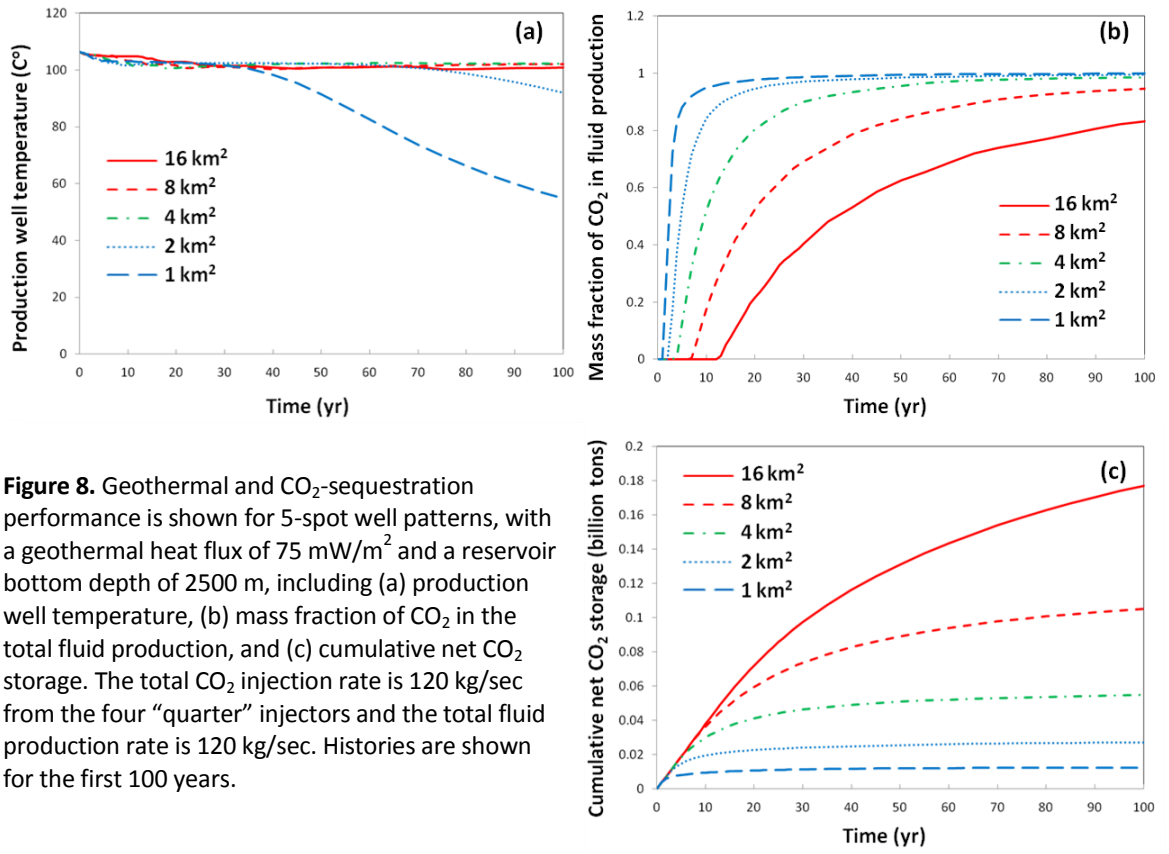

Figure 8. Geothermal and CO_2-sequestration performance is shown for 5-spot well patterns, with a geothermal heat flux of 75 mW/m^2 and a reservoir bottom depth of 2500 m, including (a) production well temperature, (b) mass fraction of CO_2 in the total fluid production, and (c) cumulative net CO_2 storage. The total CO_2 injection rate is 120 kg/sec from the four "quarter" injectors and the total fluid production rate is 120 kg/sec. Histories are shown for the first 100 years.

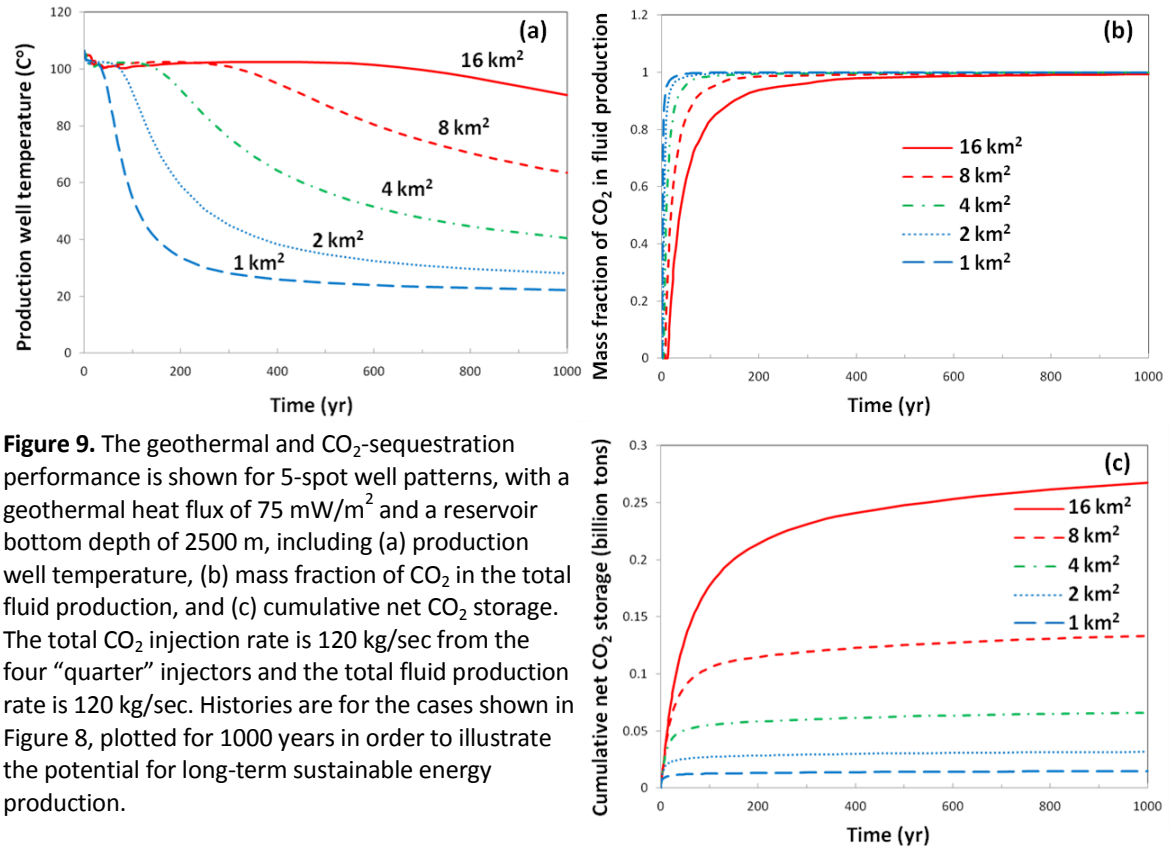

Figure 9. The geothermal and CO_2-sequestration performance is shown for 5-spot well patterns, with a geothermal heat flux of 75 mW/m^2 and a reservoir bottom depth of 2500 m, including (a) production well temperature, (b) mass fraction of CO_2 in the total fluid production, and (c) cumulative net CO_2 storage. The total CO_2 injection rate is 120 kg/sec from the four "quarter" injectors and the total fluid production rate is 120 kg/sec. Histories are for the cases shown in Figure 8, plotted for 1000 years in order to illustrate the potential for long-term sustainable energy production.

Figures 8b and 9b show the influence of well spacing on CO_2 breakthrough time and CO_2 mass fraction in the production wells. Figures 8c and 9c show the influence that CO_2 breakthrough and mass fraction have on cumulative net CO_2 storage. At 30 years, the percentage of injected CO_2 that is permanently stored is 10.2, 21.3, 40.8, 65.0, and 85.9 percent for well spacings of 0.7071, 1.0, 1.4142, 2.0, and 2.8284 km, respectively (Table 7). At 100 years, the percentage of injected CO_2 that is permanently stored is reduced: 3.3, 7.2, 14.6, 27.7, and 46.7 percent for well spacings of 0.7071, 1.0, 1.4142, 2.0, and 2.8284 km, respectively.

To investigate the influence of reservoir thickness on economic lifetime, we analyzed the case with 2.8284-km well spacing for reservoir thicknesses of 250 and 125 m (Figure 10 and Tables 8 and 9). Compared to the 250-m-thick-reservoir case, the injected CO_2 for the 125-m-thick-reservoir case has half the residence time between the CO_2 injectors and the producer. Consequently, the CO_2 plume arrives at the producer before it is has time to be heated to close to formation temperature, causing a slightly greater thermal drawdown at 30 years than in the 250-m-thick-reservoir case (4^oC versus 1^oC). Subsequently, thermal conduction heats the CO_2 plume, increasing the temperature to close to formation temperature (nearly reaching a steady state), with minimal thermal drawdown (1^oC) at 100 and 200 years for the 125-m-thick-reservoir case. Thereafter, the thermal drawdown gradually becomes slightly greater than in 250-m-thick-reservoir case (Table 8), resulting in an economic lifetime is somewhat less than that of the 250-m-thick-reservoir case (750 versus 950 years).

Figure 10b shows the influence of reservoir thickness on CO_2 breakthrough time and CO_2 mass fraction in the production wells. Figure 10c show the influence that CO_2 breakthrough and mass fraction have on cumulative net CO_2 storage. During the first 10 years, cumulative net storage is similar (Table 9); thereafter, the ratio of cumulative net CO_2 storage approaches two, directly proportional to the relative reservoir thickness.

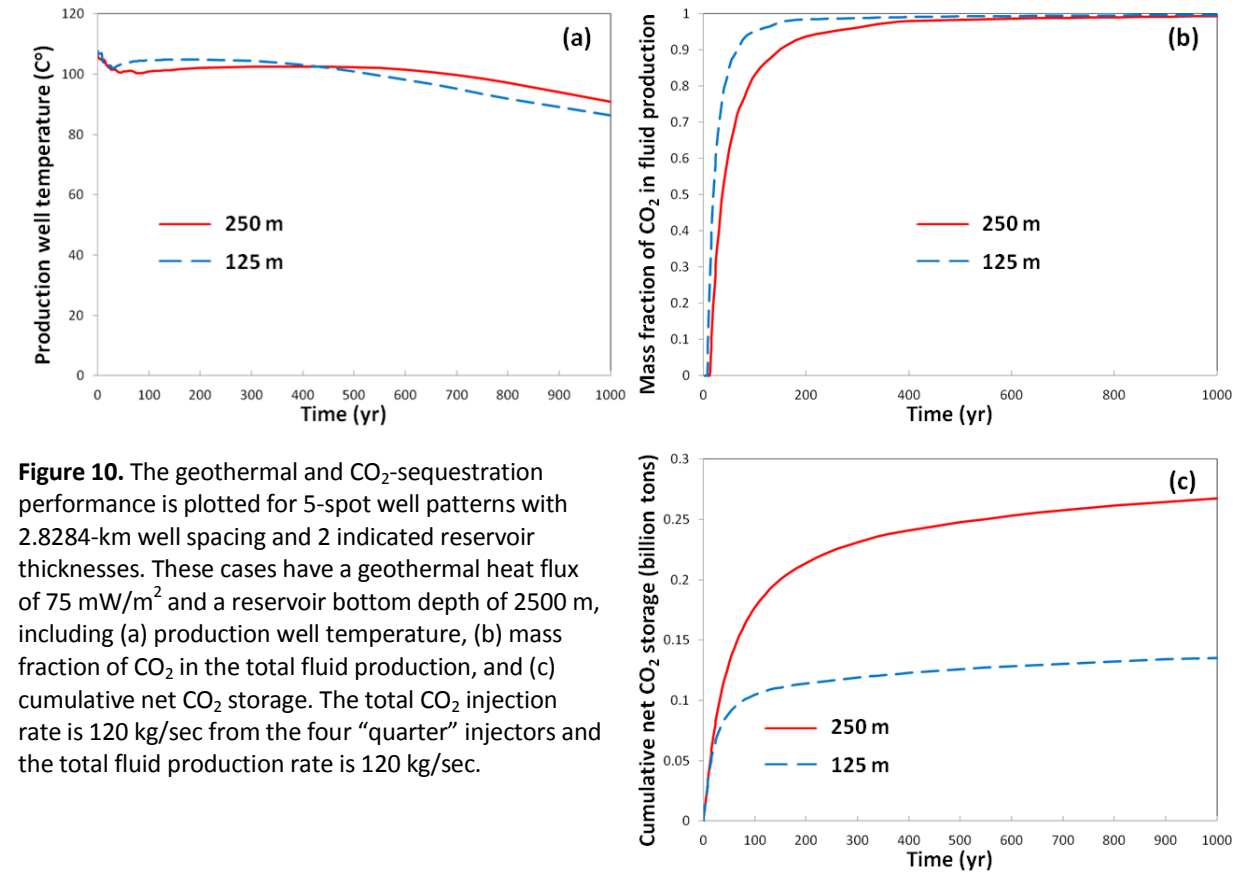

Figure 10. The geothermal and CO_2-sequestration performance is plotted for 5-spot well patterns with 2.8284-km well spacing and 2 indicated reservoir thicknesses. These cases have a geothermal heat flux of 75 mW/m^2 and a reservoir bottom depth of 2500 m, including (a) production well temperature, (b) mass fraction of CO_2 in the total fluid production, and (c) cumulative net CO_2 storage. The total CO_2 injection rate is 120 kg/sec from the four "quarter" injectors and the total fluid production rate is 120 kg/sec.

Table 8. Production well temperature histories are summarized for a 5-spot well pattern with 2.8284-km well spacing (Figure 10).

Reservoir thickness (m)	Production temperature (°C)								Thermal drawdown (°C)[a]					
	0 yr	10 yr	30 yr	50 yr	100 yr	200 yr	500 yr	1000 yr	30 yr	50 yr	100 yr	200 yr	500 yr	1000 yr
250 m	106.0	103.0	102.0	102.0	102.0	102.0	102.0	90.9	1.0	1.0	1.0	1.0	1.0	12.1
125 m	108.0[b]	106.0	102.0	103.0	105.0	105.0	101.0	86.3	4.0	3.0	1.0	1.0	5.0	19.7

[a]Thermal drawdown is determined relative to the temperature at 10 yr, because the initial temperature decline is caused by drawing cooler brine from the upper half of the reservoir. Thermal drawdown is 10.8°C at 750 years for the 125-m-thick-reservoir case and is 10.6°C at 950 years for the 250-m-thick-reservoir case.

[b]Initial temperature is higher than in the 250-m-thick reservoir because the average reservoir depth is 62.5 m greater.

Table 9. CO_2-sequestration performance is summarized for a 5-spot well pattern with 2.8284-km well spacing (Figure 10).

Reservoir thickness (m)	Cumulative net CO_2 storage (million tons)							
	0 yr	10 yr	30 yr	50 yr	100 yr	200 yr	500 yr	1000 yr
250 m	0.0	37.9	97.6	131.0	177.0	214.0	248.0	267.0
125 m	0.0	36.9	74.8	89.7	105.0	114.0	126.0	135.0

7. Future Work

In this report we introduced and analyzed a two-stage, integrated geothermal-CCS approach. In future work, we will investigate various permutations and extensions of this approach, with an emphasis on options for the reinjection of either produced brine or residual brine that is blowdown from either RO desalination or saline-cooling operations. In considering brine reinjection options, we will introduce and analyze a three-stage, integrated geothermal-CCS approach. In the three-stage approach, stage one will involve the reinjection of produced brine, rather than CO_2 injection; thus, brine will be re-circulated as the working fluid. One of the purposes of stage one will be to characterize the reservoir, possibly involving the use of smart tracers, to investigate reservoir heterogeneity and compartmentalization, while producing a revenue stream for the integrated geothermal-CCS operation. This would allow for the determination of the tendency for fast pathways and for the natural loss (i.e., attrition) of working fluid during injection/production operations, which reduces the uncertainty about the economic viability of the subsequent stages. Stage two could be a modification of stage one (see Section 4), wherein CO_2 is gradually introduced as an injected working fluid, perhaps functioning as a make-up fluid to address the *natural attrition* of reinjected brine. Stage two will also involve the *engineered attrition* of brine, wherein brine is diverted for some consumptive beneficial use (see Section 3.1), which allows for increased CO_2 injection rates, while remaining within a *pressure-management target* for sequestration security. Finally, stage three would be an extension of stage two (see Section 4), with the addition of brine or residual brine reinjection.

8. Summary and Conclusions

The challenges of mitigating global climate change and generating sustainable energy are inseparable and require innovative, cross-cutting thinking that aggressively seeks synergistic opportunities in an open-minded manner. We conducted a preliminary reservoir engineering analysis of a two-stage, integrated geothermal-CO_2-storage approach, which can be flexibly deployed to optimize the combination of geothermal energy recovery and secure CO_2 sequestration, at reduced environmental risk. The conceptual model used in this study is highly idealized. Real reservoir systems will be heterogeneous, with the storage formation possibly being compartmentalized, and with regions of lower permeability than used in this example. These conditions are likely to require more complex well configurations that adapt and conform to the permeability structure of the reservoir. Heterogeneity will result in earlier CO_2 breakthrough than shown in our examples, which will reduce the duration of stage one, and enable earlier utilization of CO_2 as a working fluid. The results of this study are quite encouraging with regards to large-scale, secure CO_2 sequestration and to sustainable geothermal energy recovery and should motivate further reservoir, geospatial, and economic investigations of various permutations and extensions of this approach.

Acknowledgements

This work was sponsored by USDOE Geothermal Technologies Program and by the Carbon Mitigation Initiative at Princeton University and by the Environmental Protection Agency under Cooperative Agreement RD-83438501. The authors acknowledge the review of Pat Berge at Lawrence Livermore National Laboratory (LLNL). This work was performed under the auspices of the U.S. Department of Energy by LLNL under contract DE-AC52-07NA27344.

References

Aines, R.D., Wolery, T.J., Bourcier, W.L., Wolfe, T, and Haussmann, C.W., 2011. Fresh water generation from aquifer-pressured carbon storage: Feasibility of treating saline formation waters, *Energy Procedia,* 4, 2269–2276.

ASME, 2006. ASME Steam Tables Compact Edition, ASME, Three Park Avenue, New York, NY, USA.

Bergmo, P.E.S., Grimstad, A-A., and Lindberg, E., 2011. Simultaneous CO_2 injection and water production to optimize aquifer storage capacity, *International Journal of Greenhouse Gas Control*, 5, 555-564.

Birkholzer, J.T. and Zhou, Q., 2004. Basin-scale hydrogeologic impacts of CO_2 storage: Capacity and regulatory implications, *International Journal of Greenhouse Gas Control* 3, 745-756, 2009.

Blackwell, D.D, and Richards, M. Geothermal Map of North America. American Association of Petroleum Geologists, Tulsa, Oklahoma, 1 sheet, scale 1:6,500,000.

Brown, D.W., 2000. A hot dry rock geothermal energy concept using supercritical CO_2 instead of water. *Proceedings of the Twenty-Fifth Workshop on Geothermal Reservoir Engineering*, Stanford University, pp. 233-238.

Bourcier, W.L., Wolery, T.J., Wolfe, T., Haussmann, C., Buscheck, T.A., and Aines, R.D., 2011. A preliminary cost and engineering estimate for desalinating produced formation water associated with carbon dioxide capture and storage, *International Journal of Greenhouse Gas Control*, 5, 1319-1328.

Buscheck, T.A., Glascoe, L.G., Lee, K.H., Gansemer, J., Sun, Y., and Mansoor, K., 2003. Validation of the multiscale thermohydrologic model used for analysis of a proposed repository at Yucca Mountain, Journal of Contaminant Hydrology, 62 (3), 421–440.

Buscheck, T.A., 2010. Active management of integrated geothermal-CO_2-storage reservoirs in sedimentary formations: An approach to improve energy recovery and mitigate risk, Proposal in response to DE_FOA-0000336: Energy Production with Innovative Methods of Geothermal Heat Recovery, LLNL-PROP-463758.

Buscheck, T.A, Sun, Y., Hao, Y., Wolery, T.J., Bourcier, W.L., Tompson, A.F.B., Jones, E.D., Friedmann, S.J., and Aines, R.D., 2011a. Combining brine extraction, desalination, and residual-brine reinjection with CO_2 storage in saline formations: Implications for pressure management, capacity, and risk mitigation, *Energy Procedia* 4, 4283–4290.

Buscheck, T.A., Sun, Y., Hao, Y., Chen, M., Court, B., Celia, M.A., and Wolery, T. J. 2011b. Geothermal energy production from actively-managed CO_2 storage in saline formations, Proceedings for the Geothermal Resources Council 35th Annual Meeting: 23–26 October 2011, San Diego, CA, USA.

Buscheck, T.A., Sun, Y., Chen, M., Hao, Y., Wolery, T.J., Bourcier, W.L., Court, B., Celia, M.A., Friedmann, S.J., and Aines, R.D., 2012a. Active CO_2 reservoir management for carbon storage: analysis of operational strategies to relieve pressure buildup and improve injectivity, *International Journal of Greenhouse Gas Control*, 6, 230-245, doi:10.1.1016/j.ijggc.2011.11.007.

Buscheck, T.A., Sun, S., Chen, M., Hao, Y., Wolery, T.J., Friedmann, S.J., and Aines, R.D., 2012b. Active CO_2 reservoir management for CO_2 capture, utilization, and storage: An approach to improve CO_2 storage capacity, and to reduce risk, CMTC 151746, Proceedings for the Carbon Management Technology Conference, 7–9 February, 2012, Orlando, FL, USA.

Buscheck, T.A., Chen, M., Sun, Y., Hao, Y., Wolery, T.J., and Aines, R.D., 2012c. Active CO_2 reservoir management: Analysis of strategies to increase CO_2 storage capacity and to reduce pore-space competition with neighboring subsurface activities, proceedings of the 11th Annual Conference on Carbon Capture, Utilization, and Sequestration, April 30–May 3, 2012, Pittsburgh, PA, USA.

Carroll, S., Hao, Y., and Aines, R.D., 2008. Transport and detection of carbon dioxide in dilute aquifers. In Proceedings for the 9th International Conference on Greenhouse Gas Control Technologies: 16-20 November 2008, Washington DC, USA.

Carroll, S.A., Hao, Y., and Aines, R.D., 2009. Geochemical detection of carbon dioxide in dilute aquifers. *Geochemical Transactions* 10, 4.

Court, B., Elliot, T. R., Dammel, J., Buscheck, T.A., Rohmer, J., Celia, M.A., 2011a. Promising synergies to address water, sequestration, legal, and public acceptance issues associated with large-scale implementation of CO_2 sequestration, Special Issue on Carbon Capture and Storage (CCS) "Five years after the IPCC Special Report on CCS: state of play, *Mitigation and Adaptation of Strategies for Global Change Journal*, DOI 10.1007/s11027-011-9314-x.

Court, B., Celia, M.A., Nordbotten, J.M., and Elliot, T.R., 2011b. Active and integrated management of water resources throughout CO_2 capture and sequestration operations, *Energy Procedia*, 4, 4221–4229.

Court, B., Bandilla, K., Celia, M.A., Buscheck, T.A., Nordbotten, J.M., Dobossy, M., and Jansen, A., 2012. Initial evaluation of advantageous synergies associated with simultaneous brine production and CO_2 geological sequestration, *International Journal of Greenhouse Gas Control*, accepted for publication.

Court, B., "Safety and water challenges in CCS: Modeling studies to quantify CO_2 and brine leakage risk and evaluate promising synergies for active and integrated water management", PhD Dissertation, Princeton University, 2011. Available at http://dspace.princeton.edu/jspui/handle/88435/dsp01ms35t861f.

Duke, D., 2007. ZLD: New silica based inhibitor chemistry permits cost effective water conservation for HVAC and industrial cooling towers, IWC Report 07-11, Proceedings for the 69th Annual International Water Conference, October 26-29, 2008, San Antonio, Texas.

Elliot, T.R. and Celia, M.A. 2012. Potential restrictions to CO_2 sequestration sites due to shale and tight gas production. *Environmental Science & Technology*, accepted.

Elliot, T.R., Buscheck, T.A., and Celia, M.A., 2012. Active CO_2 reservoir management: A two-stage approach for sustainable geothermal energy production with reduced risk of brine leakage and increased CO_2 security, proceedings of the 11th Annual Conference on Carbon Capture, Utilization, and Sequestration, April 30–May 3, 2012, Pittsburgh, PA, USA.

Fenghour, A., Wakeham, W.A., and Vesovic, V, 1998. The viscosity of carbon dioxide. *J. Phys. Chem. Ref. Data*, **27**, 1, 31-44.

Glanz, J., Deep in bedrock, clean energy and quake fears, New York Times, June 23, 2009.

Harto, C.B. and Veil, J.A., 2011. Management of water extracted from carbon sequestration projects. Argonne National Laboratory, ANL/EVS/R-11/1.

IPCC, 2005. IPCC. Special Report on carbon dioxide capture and storage. Cambridge University Press.

Johnson, J.W., Nitao, J.J., Knauss, K.G., 2004a. Reactive transport modeling of CO_2 storage in saline aquifers to elucidate fundamental processes, trapping mechanisms and sequestration partitioning. In: Baines, S.J., Worden, R.H. (Eds.), Geological Storage of Carbon Dioxide. Special Publications, vol. 223. Geological Society, London, 107–128.

Johnson, J.W., Nitao, J.J., Morris, J.P., 2004b. Reactive transport modeling of cap rock integrity during natural and engineered CO_2 storage. In: Benson, S. (Ed.), CO_2 Capture Project Summary, vol. 2. Elsevier.

Maulbetsch, J.S., and M.N. DiFilippo. 2010. *Performance, Cost, and Environmental Effects of Saltwater Cooling Towers*. California Energy Commission, PIER Energy-Related Environmental Research Program. CEC-500-2008-043. http://www.energy.ca.gov/2008publications/CEC-500-2008-043/CEC-500-2008-043.pdf.

MIT, 2006. The Future of Geothermal Energy: Impact of Enhanced Geothermal Energy Systems (EGS) in the United States in the 21st Century, 2006.

Morris J.P., Detwiler, R.L., Friedmann, S.J., Vorobiev, O.Y., and Hao, Y., 2011. The large-scale geomechanical and hydrological effects of multiple CO_2 injection sites on formation stability, *International Journal of Greenhouse Gas Control* 5, 69-74.

Nitao, J.J., 1998. "Reference manual for the NUFT flow and transport code, version 3.0," Lawrence Livermore National Laboratory, UCRL-MA-130651-REV-1.

Pruess, K., 2006. Enhanced geothermal systems (EGS) using CO_2 as working fluid – a novel approach for generating renewable energy with simultaneous sequestration of carbon. *Geothermics* v. 35, pp. 351-367.

Randolph, J.B. and Saar, M.O. 2011a. Coupling carbon dioxide sequestration with geothermal energy capture in naturally permeable, porous geologic formations: Implications for CO_2 sequestration. *Energy Procedia* 4, 2206–2213.

Randolph, J.B. and Saar, M.O. 2011b. Impact of reservoir permeability on the choice of subsurface geothermal heat exchange fluid: CO_2 versus water and native brine. Proceedings for the Geothermal Resources Council 35th Annual Meeting: 23–26 October 2011, San Diego, CA, USA.

Socolow, R.H. and Pacala, S.W., 2006. A plan to keep carbon in check, *Scientific American*, vol. 295, no.3, pp.50-57.

Span, R., and Wagner, W., 1996. A new equation of state for carbon dioxide covering the fluid region from the triple-point temperature to 1100K at pressures up to 800 MPa. *Journal of Physical and Chemical Reference Data* 25, 1509–1596.

Surdam, R.C., and Jioa, Z., 2007. "The Rock Springs Uplift: An outstanding geological CO_2 sequestration site in southwest Wyoming," Wyoming State Geological Survey, Challenges in Geologic Resource Development No. 2.

Surdam, R.C, Jiao, Z, Stauffer, P, and Miller, T., 2009. "An integrated strategy for carbon management combining geological CO_2 sequestration, displaced fluid production, and water treatment," Wyoming State Geological Survey, Challenges in Geologic Resource Development No. 8.

van Genuchten, M.T., 1980. A closed form equation for predicting the hydraulic conductivity of unsaturated soils. *Soil Science Society of America Journal*, 44: 892-898.

Zhou, Q., Birkholzer, J.T., Tsang C-F., and Rutqvist, J. A., 2008.A method for quick assessment of CO_2 storage capacity in closed and semi-closed saline formations. *International Journal of Greenhouse Gas Control* 2, 626-639.